

Nature of inhomogeneous magnetic state in artificial Fe/Gd ferrimagnetic multilayers

D. Haskel,¹ G. Srajer,¹ Y. Choi,¹ D. R. Lee,¹ J. C. Lang,¹ J. Meersschant,² J. S. Jiang,² and S. D. Bader²

¹Advanced Photon Source, Argonne National Laboratory, Argonne, Illinois 60439, USA

²Materials Science Division, Argonne National Laboratory, Argonne, Illinois 60439, USA

(Received 28 March 2003; published 29 May 2003)

The low-field surface nucleation and evolution of the inhomogeneous magnetic state in strongly coupled Fe/Gd ferrimagnetic multilayers is measured via grazing-incidence x-ray magnetic circular dichroism. At $T \approx 0.7 T_0$, where $T_0 \sim 110$ K is the ferrimagnetic compensation temperature, the inhomogeneous state nucleates at the surface. At nucleation, the surface state extends tens of interatomic distances into the bulk (≈ 200 Å), a direct consequence of the strong interlayer coupling. At $T \sim T_0$, the inhomogeneous state penetrates throughout the bulk, while homogeneous magnetic states occur far below and above T_0 . Surface termination has a dramatic effect on the nature of the inhomogeneous state.

DOI: 10.1103/PhysRevB.67.180406

PACS number(s): 75.70.-i, 75.25.+z, 75.75.+a

Understanding the physical interactions that lead to spatially inhomogeneous magnetic ground states remains a challenge for theorists and experimentalists alike. In this respect artificial magnetic nanostructures have proven to be unique model systems, resulting in significant advances in this area. For example, symmetry breaking at surfaces of Fe/Cr artificial antiferromagnets and biquadratic coupling in exchange Fe/SmCo soft/hard ferromagnets induce novel inhomogeneous ground states.^{1,2} The role of broken symmetry at surfaces and interfaces as a source for chiral effects in magnetic nanostructures has recently been investigated theoretically.³

Fe/Gd artificial ferrimagnets have been used as model systems in several investigations.^{4,5} The markedly different bulk Curie temperatures of Fe (1024 K) and Gd (293 K), together with strong interlayer antiferromagnetic coupling at the Fe/Gd interface, result in a rich phase diagram with magnetic configurations that strongly depend on applied field and temperature.⁴ Although experimental evidence for a magnetic inhomogeneous state has been gathered by several techniques,⁵ a long-standing key issue on the mechanism of nucleation of such state has not been resolved experimentally until now. Over a decade ago LePage and Camley⁶ predicted that a phase transition into an inhomogeneous magnetic state would nucleate at the surface of a strongly coupled artificial ferrimagnetic multilayer if the multilayer is terminated by the minority magnetic component. In this “surface-twisted” phase, the magnetization deviates from the applied field direction near the surface while the bulk remains field aligned. This inhomogeneous phase has eluded direct experimental detection due to the difficulty in probing surface and bulk states in the same measurement. The challenge is to observe both the existence of a surface-twisted phase and the absence of a bulk twist. Inhomogeneous magnetic depth profiles in layered nanostructures are commonly probed by scattering techniques (reciprocal space) such as neutron reflectometry⁷ and x-ray resonant magnetic scattering.⁸ Although these are powerful probes of magnetism, the measurement of the scattered intensity often results in model-dependent magnetization profiles. In addition, Gd is a strong neutron absorber and, therefore, bulk sensitivity is reduced in neutron measurements.

In this Communication, we report *direct*, real-space, measurements of the low-field nucleation of an inhomogeneous magnetic state at the surface of a Fe-terminated $[\text{Fe}(35 \text{ \AA})/\text{Gd}(50 \text{ \AA})]_{15}/\text{Fe}(35 \text{ \AA})$ ferrimagnetic multilayer. We exploit the penetration depth tunability of x rays at grazing- and larger-incidence angles to alternately probe the surface and the bulk magnetic states by x-ray magnetic circular dichroism (XMCD).⁹ At $T \approx 0.7 T_0$, where $T_0 \sim 110$ K is the ferrimagnetic compensation temperature at which the sublattice magnetizations are equal but opposite, the magnetic twist nucleates at the surface but penetrates ≈ 200 Å (two to three bilayers) into the bulk as a result of strong Fe/Gd interlayer exchange coupling. The reduction in Zeeman energy as T_0 is approached from below causes the inhomogeneous state to propagate throughout the bulk. Surface nucleation is not observed for a Gd-terminated multilayer showing that surface termination plays a crucial role in defining the magnetic ground state. The results are in excellent agreement with theoretical predictions and help elucidate the driving forces behind inhomogeneous magnetic state nucleation in artificial ferrimagnets.

The multilayers were sputtered onto Si substrates using Nb buffer (100 Å) and cap (30 Å) layers. Superconducting quantum interference device (SQUID) magnetometry shows, and XMCD measurements confirm, that the multilayers couple antiferromagnetically at the Fe/Gd interfaces and have coercive fields < 50 Oe at 300 K. X-ray measurements were performed at sector 4 of the Advanced Photon Source at Argonne National Laboratory. Undulator radiation was monochromatized with double Si(111) crystals and its polarization converted from linear to circular with a diamond (111) quarter-wave plate operated in Bragg transmission geometry.¹⁰ A closed-cycle He refrigerator, mounted on the ϕ circle of a diffractometer, was used for the temperature-dependent measurements. The sample was placed between the pole pieces of an electromagnet delivering magnetic fields in the range of ± 600 Oe in a direction parallel to the sample's surface and nearly coincident with the x-ray wave vector.

The experimental setup permits simultaneous measurements of specular reflectivity and XMCD in fluorescence geometry. Figure 1 shows the sum ($\mu_f^+ + \mu_f^-$) and asymmetry

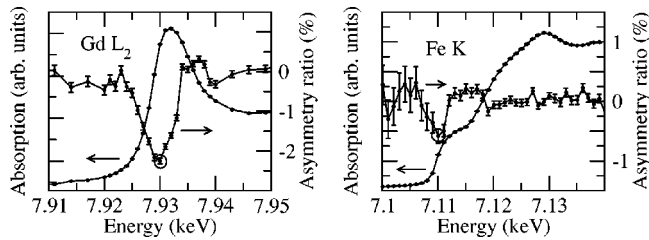


FIG. 1. Absorption and asymmetry ratios near Gd L_2 and Fe K absorption edges measured at $T=20$ K, $H=600$ Oe and $\theta_i=9.5^\circ$ on a Fe-terminated multilayer. Optimal energies used for element-specific hysteresis loops are those that maximize the magnetic contrast (circles).

ratio $(\mu_f^+ - \mu_f^-)/(\mu_f^+ + \mu_f^-)$ of fluorescence signals, measured near the Gd L_2 ($2p_{1/2}$) and Fe $K(1s)$ absorption edges (+ and - denote opposite helicities of circularly polarized x rays). While the sum is proportional to the sample's absorption coefficient, the asymmetry ratio is proportional to the element-specific magnetization. Element-specific hysteresis loops were then measured at the resonant energies for which the magnetic contrast is the largest (7.93 and 7.11 keV for Gd and Fe, respectively) by reversing the x-ray helicity at each applied field value and measuring the asymmetry ratio.

The specularly reflected signal was used to accurately determine the x-ray incidence angle. This is important since the penetration depth varies rapidly for $\theta_i > \theta_c(E)$, where $\theta_c(E)$ is the critical angle for total external reflection. The angle used to enhance surface sensitivity, $\theta_i=0.43^\circ$, is slightly above the critical angle $\theta_c \sim 0.35^\circ$ (see Ref. 11). Further decreasing the incidence angle towards θ_c was not practical,

since the Nb cap and Fe layers (above Gd) and Nb cap layer (above Fe) transfer intensity from absorption to scattering channels degrading the fluorescence signal-to-noise ratio. Despite these structural constraints, which are typical in magnetic heterostructures, we were able to retrieve surface-enhanced magnetic information from Gd layers. At the Fe resonance, surface sensitivity was reduced due to smaller absorption in Gd layers (below Gd $L_{2,3}$ edges) and Fe layers (resonance occurs near the bottom of the Fe absorption edge) (Fig. 1).¹² A Parratt fit to the specular reflectivity data (modified to include roughness) confirmed the nominal structural parameters of the multilayer.¹³

Gd and Fe hysteresis loops for selected temperatures below, near, and above T_0 in a Fe-terminated multilayer are shown in Fig. 2 (left). For the Gd loops, at each temperature, two sets of data are shown corresponding to surface-enhanced loops at $\theta_i=0.43^\circ$ (probes approximately two bilayers) and bulk-sensitive loops at $\theta_i=9.5^\circ$ (probes the whole multilayer). We did not detect significant differences between Fe loops at these angles due to the diminished surface sensitivity at the Fe resonance and the larger error bars associated with the smaller dichroic signal, so we only show bulk-sensitive Fe loops. Since XMCD is proportional to the projection of the magnetization along the x-ray wave vector, a “flat” hysteresis loop in Fig. 2 indicates that this projection remains unchanged as a function of H . This is the situation at 10 K, where Gd dominates the Zeeman energy and aligns with H , while Fe is constrained antiparallel by interlayer exchange. At 70 and 90 K, increasingly “tilted” Gd loops are measured at the top part of the multilayer, while bulk-sensitive Gd loops show less tilting. Tilting indicates a de-

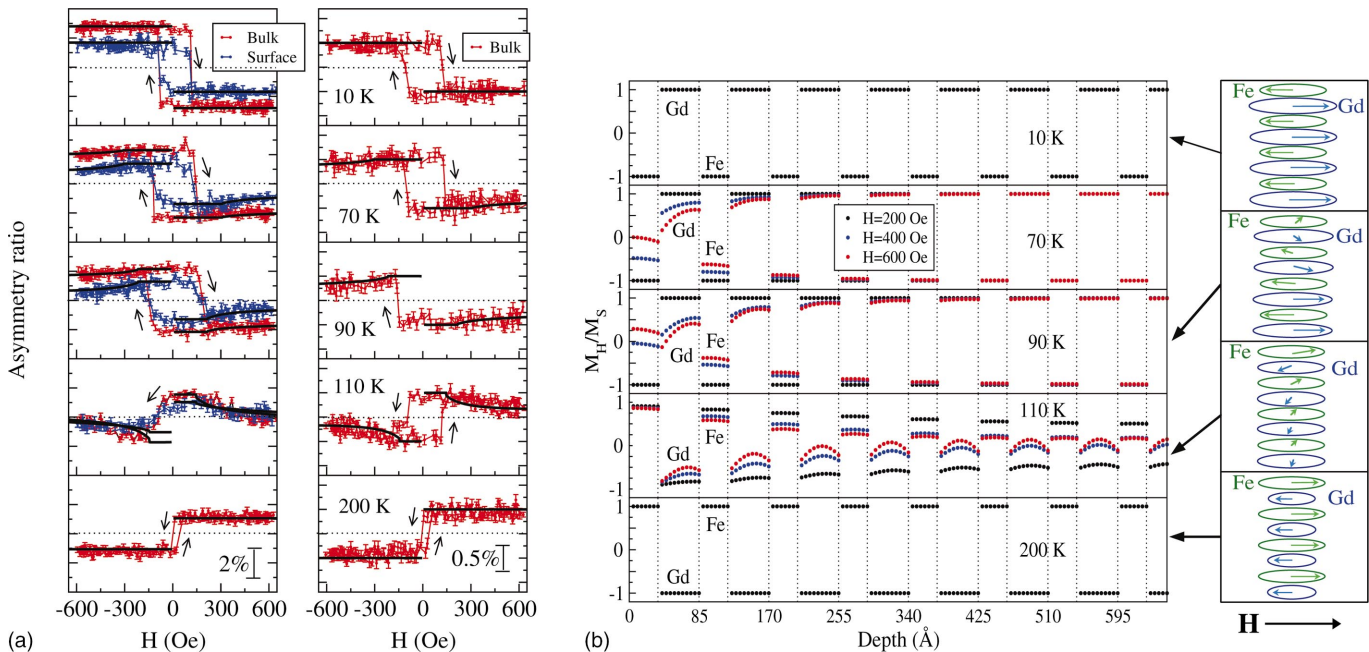


FIG. 2. (Color) Left panel: Gd (left) and Fe (right) hysteresis loops (points). Surface-sensitive loops are scaled down for clarity. Solid lines through the data are obtained from theoretical magnetization depth profiles (right panel). Theoretical results are shown for half of the multilayer structure; other half is mirror symmetric. Here, the magnetization is normalized to the saturation magnetization at each temperature. The schematic diagram (far right) represents the magnetization (intralayer averaged) in the upper four bilayers at the different temperatures and $H=600$ Oe.

crease in the projection of the moment along H ; i.e., a gradual twist of the probed magnetization away from the field direction. At 110 K, the tilting or twist already propagates throughout the multilayer, as evidenced from the now significantly tilted bulk loops. A correlated reversal in the sign of Gd and Fe loops at this temperature indicates that the Fe magnetization now dominates the Zeeman energy contribution with its net component, averaged over depth, having a positive projection along the field. At 200 K, the loops are again flat, with the Fe aligning along the field and Gd antiparallel to it.

The hysteresis loops of Fig. 2 can be classified, following Camley,⁴ as (a) Gd-aligned, (b) surface-twisted, (c) bulk-twisted, and (d) Fe-aligned phases. These phases are predicted to emerge as a result of a delicate balance between intralayer and interlayer exchange and Zeeman energies. A deviation from a collinear, antiparallel arrangement of the Gd and Fe magnetizations along H can only be driven by a reduction in Zeeman energy, since the exchange energy is already minimized in the collinear arrangement. In order to be energetically favorable, a twist configuration has to satisfy the Zeeman energy “boundary” $|M_{\text{Gd}}(T)\cos\alpha_{\text{Gd}} - M_{\text{Fe}}\cos\alpha_{\text{Fe}}| > |M_{\text{Gd}}(T) - M_{\text{Fe}}|$, where $\alpha_{\text{Gd}}, \alpha_{\text{Fe}}$ are depth-averaged twist angles. A gain in the *difference* between the projected magnetizations along H has to take place for a twist to occur. Here, the T dependence in the magnitude of the Gd magnetization is explicitly noted, while that of Fe is neglected. For $M_{\text{Gd}} > M_{\text{Fe}}$, this can only be satisfied if $\alpha_{\text{Fe}} > \alpha_{\text{Gd}}$; i.e., the “minority” sublattice has to twist more than the “majority” sublattice in order to compensate for the increased Zeeman energy of the latter. These different twist angles, however, result in an increased exchange energy, either due to deviations from antiferromagnetic alignment at the Fe/Gd interfaces or deviations from ferromagnetic alignment within the Fe and Gd layers themselves. It is the competition between this increased exchange energy and the reduction in Zeeman energy that determines the magnetic ground state.

At 10 K, $M_{\text{Gd}} \approx 1.55M_{\text{Fe}}$,¹⁴ and a twist would be too costly in exchange, favoring a Gd-aligned phase. At 70 and 90 K, the spontaneous Gd magnetization is lowered by ≈ 20 –25%, as seen from the reduced Gd hysteresis jump, resulting in $M_{\text{Gd}} \approx 1.20(4)M_{\text{Fe}}$. Under these conditions, the magnetization twists away from H only at the top (and bottom) of the multilayer, while the interior remains field aligned. For example, at 90 K the Gd surface-sensitive XMCD is reduced by $\sim 65\%$ at $H=600$ Oe, while the bulk XMCD decreases only by $\sim 20\%$. Considering the probing depth of approximately two bilayers at $\theta_i=0.43^\circ$,¹³ and given that top and bottom parts of the multilayer are equivalent, the average reduced magnetization m in the inner ~ 11 bilayers can be obtained from $[0.35 \times 4 + 11m]/15 = 0.8$. This yields $m=0.96$; i.e., the interior of the multilayer remains mostly field aligned. The reduction in the bulk XMCD at 70 and 90 K is mainly due to the surface contribution.

It is instructive to compare the experimental results with theoretical calculations of the static magnetization profile. The Landau-Lifshitz equation of motion with energy dissipation is an efficient and robust energy minimization scheme

that is very often used in micromagnetic calculations.¹⁵ We implemented this approach to obtain static solutions of the one-dimensional spin chain, as described in Ref. 16. The chain consisted of 262 sites as the Fe and Gd layers were artificially divided into seven and ten sublayers, respectively. Ferromagnetic exchange coupling in Fe and Gd layers were scaled to their bulk T_C , $J_{\text{Gd}}=0.28J_{\text{Fe}}$, while interlayer antiferromagnetic exchange was set to $-(J_{\text{Fe}}+J_{\text{Gd}})/2 = -0.64J_{\text{Fe}}$ (alloy mean-field calculations⁴ yield $-0.706J_{\text{Fe}}$). The saturation magnetization $M_s(T)$ in Gd layers was independently obtained from integrated areas of angle-dependent XMCD measurements and T -dependent hysteresis jumps. Results from these calculations are shown in the right panel of Fig. 2. The surface nucleation of the inhomogeneous state is clearly observed. To compare with the experimental data, the calculated magnetization depth profiles were weighted, each element separately, to account for the depth selectivity of our XMCD measurements at the different incidence angles, $\langle M \rangle_{\theta_i}(H) = \sum_l M_l(H) W_l / \sum_l W_l$, where $W_l = e^{-\mu_l z_l / \sin\theta_i}$ and $\mu_l z_l = \sum_{j \leq l} \mu_j z_j$, i.e., the compounded absorption coefficient at depth z_l (for surface-sensitive averaging we used the refracted angle $\theta_r=0.25^\circ$, see Ref. 12). The results of this averaging are shown by solid lines in the left panel of Fig. 2, where the agreement with experiment supports the conclusion of the extent of the penetration depth at nucleation. This is an important result, as previous attempts to determine the penetration depth placed it at several thousand angstroms.¹⁷

The energy barrier for a twist of the minority sublattice (Fe) towards the applied field direction H is decreased at the surface due to the absence of Fe/Gd interlayer exchange coupling at the end sides of terminal Fe layers. This results in surface nucleation of the inhomogeneous state, while the increased exchange energy cost in the bulk does not allow the twist to penetrate past the first few Fe/Gd bilayers. We had mentioned that for $M_{\text{Gd}} > M_{\text{Fe}}$, the minority sublattice has to twist more toward H than the majority sublattice twists away from it. This is seen in the data by the larger XMCD reduction, with H , in the Fe versus Gd *bulk*-sensitive loops at 70–90 K, also confirmed by the calculations. The calculations also show that most of the exchange cost associated with the inhomogeneous state is within the Gd layers (right, Fig. 2), as expected due to the weaker Gd intralayer coupling J_{Gd} compared to J_{Fe} and the antiferromagnetic interlayer coupling J_I .

At 110 K, $M_{\text{Gd}} \approx 0.98M_{\text{Fe}}$ and the twist penetrates throughout the multilayer. Here, the nearly identical sublattice magnetizations allow for the Zeeman energy boundary inequality to be satisfied at similar (and opposite) twists of the two sublattice magnetizations. This is seen by the similar XMCD reduction, with H , in Fe and Gd bulk loops at 110 K. The low exchange-energy cost of this *locally* more collinear structure stabilizes the twisted state throughout the entire multilayer. Note that both data and simulations show that, at this T , the interior of the multilayer twists more than the surface. This is because the Fe layers already dominate the magnetization and favor an aligned structure; the twist is

now driven by the Gd minority layers. At 200 K, $M_{\text{Fe}} \approx 1.6M_{\text{Gd}}$, and the roles of Gd and Fe are reversed compared to those at 10 K. The dominant Fe magnetization aligns with H , Gd being constrained antiparallel by the interlayer exchange.

The effect of surface termination upon nucleation of the inhomogeneous state was further studied on a Gd-terminated multilayer with identical composition, i.e., $\text{Gd}(50 \text{ \AA})[\text{Fe}(35 \text{ \AA})\text{Gd}(50 \text{ \AA})]_{15}$. Here, we find no evidence for nucleation of a surface-twisted phase below T_0 . Although increasing the magnetization component of the minority sublattice (Fe) along H remains the driving force for nucleation of a twist, the energy advantage encountered at the surfaces of the Fe-terminated multilayer is no longer present. Thus the phase transition into a twisted state is a bulk phenomenon which, at low fields, is confined to the vicinity of T_0 .

In summary, we directly probed, in real space, the nucleation and evolution of an inhomogeneous magnetic state in a model artificial ferrimagnetic system with strong interlayer coupling. Nucleation occurs at the surface only when the multilayer is terminated by the minority (Fe) component. The surface state penetrates $\approx 200 \text{ \AA}$ into the bulk due to strong interlayer coupling at Fe/Gd interfaces. Our results are the first direct confirmation of the long-ago predicted inhomogeneous magnetic phase in the strongly coupled model system. Furthermore, our method opens a way towards distinguishing surface from bulk states in inhomogeneous magnetic systems.

We thank C. Kmety-Stevenson for SQUID magnetization measurements. J.M. wishes to thank the Belgian Science Foundation (F.W.O.-Vlaanderen) for financial support. Work at Argonne was supported by the U.S. Department of Energy Office of Science under Contract No. W-31-109-ENG-38.

-
- ¹D.L. Mills, Phys. Rev. Lett. **20**, 18 (1968); F. Keffer and H. Chow, *ibid.* **31**, 1061 (1973); R.W. Wang *et al.*, *ibid.* **72**, 920 (1994).
- ²V.K. Vlasko-Vlasov *et al.*, Phys. Rev. Lett. **86**, 4386 (2001).
- ³A.N. Bogdanov and U.K. Röbblers, Phys. Rev. Lett. **87**, 037203 (2001).
- ⁴R.E. Camley and D.R. Tilley, Phys. Rev. B **37**, 3413 (1988); R.E. Camley, *ibid.* **39**, 12316 (1989).
- ⁵K. Cherifi *et al.*, Phys. Rev. B **44**, 7733 (1991); W. Hahn *et al.*, *ibid.* **52**, 16041 (1995); O.F.K. McGrath *et al.*, *ibid.* **54**, 6088 (1996); M. Sajieddine *et al.*, *ibid.* **49**, 8815 (1994); A. Koizumi *et al.*, *ibid.* **61**, 14909 (2000); W. Hahn *et al.*, *ibid.* **52**, 16041 (1995).
- ⁶J.G. LePage and R.E. Camley, Phys. Rev. Lett. **65**, 1152 (1990); R.E. Camley, Phys. Rev. B **35**, 3608 (1987).
- ⁷S.G.E. te Velthuis, J.S. Jiang, S.D. Bader, and G.P. Felcher, Phys. Rev. Lett. **89**, 127203 (2002).
- ⁸N. Ishimatsu *et al.*, Phys. Rev. B **60**, 9596 (1999); D. Haskel *et al.*, Phys. Rev. Lett. **87**, 207201 (2001); J. Geissler *et al.*, Phys. Rev. B **65**, 020405 (2001).
- ⁹G. Schütz *et al.*, Phys. Rev. Lett. **58**, 737 (1987); J. Stöhr, J. Magn. Mater. **200**, 470 (1999); L.M. Garcia *et al.*, Phys. Rev. Lett. **85**, 429 (2000).
- ¹⁰J.C. Lang and G. Srajer, Rev. Sci. Instrum. **66**, 1540 (1995).
- ¹¹The Nb capping layer together with Fe and Gd resonance contributions give an effective critical angle for the multilayer, which is nearly the same (within 0.02°) at Gd L_2 and Fe K resonant energies.
- ¹²The refracted beam angle with the sample's surface is $\theta_r = \sqrt{\theta_i^2 - \theta_c^2} = 0.25^\circ$ ($\theta_i = 0.43^\circ$, $\theta_c = 0.35^\circ$). The sample's absorption length at 7.93 keV and 7.11 keV is $3.3 \mu\text{m}$ and $7.9 \mu\text{m}$, respectively (using experimental optical constants for Gd and Fe). This gives penetration depths of 144 \AA (1.7 bilayers) and 350 \AA (4.1 bilayers) at Gd L_2 and Fe K resonances, respectively. Calculations of electric-field profile inside the multilayer using Parratt's formalism and fitted structural parameters yield consistent depths for a $1/e$ decrease in intensity.
- ¹³L.G. Parratt, Phys. Rev. **95**, 359 (1954). Refined structural parameters are $t_{\text{Fe}} = 35.48(2) \text{ \AA}$, $t_{\text{Gd}} = 49.38(2) \text{ \AA}$, $\sigma_{\text{Fe/Gd}} = \sigma_{\text{Gd/Fe}} = 3.7 \text{ \AA}$ (σ is the interface roughness). Gd and Fe atomic number densities are within 3% of their bulk values.
- ¹⁴Edge-jump normalized (i.e., per atom) XMCD signals at 10 K and $H = 600 \text{ Oe}$ at Fe K and Gd L_2 resonant energies are $\mu_m/\mu_e = 0.13(2)\%$, $5.1(3)\%$, respectively, in agreement with bulk values [$\mu_m = \mu^+ - \mu^-$, $\mu_e = (\mu^+ + \mu^-)/2$]. Gd and Fe magnetizations are obtained from their bulk saturation values (2020 emu/cm^3 and 1750 emu/cm^3 , respectively) and total layer thicknesses.
- ¹⁵For example, this approach is used in the OOMMF package. See <http://math.nist.gov/oommf>.
- ¹⁶N. Papanicolaou, J. Phys.: Condens. Matter **10**, L131 (1998).
- ¹⁷M. Vaezzadeh, B. George, and G. Marchal, Phys. Rev. B **50**, 6113 (1994).